Environmental Science Advances

Accepted Manuscript

This article can be cited before page numbers have been issued, to do this please use: F. Batool, M. Zubair, F. Mahmood, M. Shahid, T. Shahzad, W. Liu, S. Hussain and A. Ullah, *Environ. Sci.: Adv.*, 2026, DOI: 10.1039/D6VA00120C.

View Article Online
DOI: 10.1039/D6VA00120C

Environmental Significance

Dyes are commonly used in the textile industry and pose a critical environmental concern because of their unregulated discharge, which releases persistent, carcinogenic, and toxic compounds into ecosystems. So, the removal of dyes from textile wastewater has become a challenge with the rising water and soil pollution. Herein, the current study was designed to compare the efficacy of *Conocarpus erectus*-derived ZnO-NPs with chemically synthesized counterparts for synthetic and real wastewater treatment, and to evaluate their potential to mitigate phytotoxicity in *Vigna radiata* under stress. This research will provide a potential use of ZnO-NPs for efficient wastewater treatment and sustainable agriculture production by bridging the gap between wastewater treatment and crop health restoration.

.

View Article Online
DOI: 10.1039/D6VA00120C

Bio- and Chemically Synthesized ZnO Nanoparticles for Textile Wastewater Treatment and Phytotoxicity Alleviation in *Vigna radiata*

Fatima Batool[a,b], Muhammad Zubair[b], Faisal Mahmood[a], Muhammad Shahid[c], Tanvir Shahzad[a], Weitao Liu[d], Sabir Hussain[a]*, Aman Ullah[b*]

[a] *Department of Environmental Sciences, Government College University Faisalabad, Faisalabad, 38000, Pakistan*

[b] *Department of Agricultural, Food & Nutritional Science, Faculty of ALES, University of Alberta 4-10 Agriculture/Forestry Centre Edmonton, AB, T6G 2P5*

[c] *Department of Bioinformatics and Biotechnology, Government College University Faisalabad, Faisalabad, 38000, Pakistan*

[d] *MOE Key Laboratory of Pollution Processes and Environmental Criteria, College of Environmental Science and Engineering, Nankai University, Tianjin 300350, China*

**: Correspondence authors*

sabirghani@gmail.com; sabir.hussain@gcuf.edu.pk

ullah2@ualberta.ca

Abstract

This study reports the development of biologically and chemically synthesized zinc oxide nanoparticles (ZnO-NPs) using the leaf extract of *Conocarpus erectus* and sodium hydroxide, respectively. The synthesized nanomaterials were characterized to determine their morphology, functional groups, and crystalline nature using SEM, FTIR, and XRD. The performance of ZnO-NPs was evaluated for the photocatalytic treatment of synthetic azo dye solutions and real textile wastewater. Furthermore, they were assessed for the mitigation of phytotoxicity in *Vigna radiata*. The results demonstrated that a lower catalyst dose of ZnO(B)-

View Article Online
DOI: 10.1039/D6VA00120C

NPs showed higher efficiency for decolorizing Congo red as compared to ZnO(C)-NPs. However, dye concentration, light sources (sunlight and UV) and reducing agents had a significant effect on decolorization rates. In actual textile wastewater treatment, ZnO(B)-NPs reduced the pH, EC, TDS, sulfate, phosphate, color intensity, and COD more efficiently than ZnO(C)-NPs, showing enhanced remediation potential. Subsequently, phototoxicity studies revealed significant improvements in seed germination, growth parameters, photosynthetic content, and antioxidative enzymatic activity in *Vigna radiata* under wastewater stress. In contrast, ZnO(B)-NPs reduced the levels of oxidative stress indicators, such as hydrogen peroxide and malondialdehyde, and increased the activities of superoxide dismutase, catalase, and peroxidase. Multivariate analyses further confirmed the consistent and better performance of ZnO(B)-NPs in wastewater remediation and plant stress alleviation response metrics. Overall, this study suggests that *Conocarpus* derived ZnO-NPs offer green and sustainable high-performance materials to mitigate textile effluent toxicity and improve crop performance under stress conditions.

Keywords: Biosynthesis; Chemical synthesis; Wastewater treatment; Phytotoxicity; *Vigna radiata*; Zinc oxide nanoparticles

1. Introduction

Water is one of the most important pillars of the environment, required not only for sustaining life on Earth but also for maintaining the balance of ecosystems. Although there are plentiful natural water resources, only a fraction of them are suitable for human consumption. Industrial activities discharge toxic organic and inorganic pollutants, such as heavy metals, dyes, salts, and other compounds, into water bodies. Among chemical industries, the textile sector is considered a major contributor, releasing huge concentrations of dyes and heavy metals into freshwater bodies without any proper treatment.[1] It has been reported that the manufacture of 1 g of fabric requires approximately 200 L of water and 90 g of dyes,

View Article Online
DOI: 10.1039/D6VA00120C

discharging 280,000 tons of dye-contaminated water into freshwater annually.[1,2] Textile wastewater contains toxic dyes, heavy metals, surfactants, anions, and other organic compounds such as azo compounds.[1,3] These non-biodegradable pollutants resist conventional treatments and persist in the environment, reducing water quality, impairing photosynthesis,and increasings chemical and biological oxygen demand.[4] This wastewater degrades agricultural land when used for irrigation, thus necessitating efficient treatment before disposal.

Conventional physicochemical methods for wastewater treatment are costly, energy-intensive, utilize toxic chemicals, and produce secondary byproducts such as sludge. [5,6] While biological methods use microorganisms[7] but less effective due to the complex nature of microorganisms and the survival challenge. Thus, the advanced oxidation process provides a great alternative for wastewater treatment by producing reactive oxygen species of superoxide and hydroxyl radicals for organic compounds oxidation.[7–10] Different photocatalysts, such as copper[11], iron[4], nickel[12] and titanium[13], generate active oxygen species under light, which react with dyes and convert them into harmless byproducts.

On the other hand, Zinc oxide nanoparticles (ZnO-NPs) are particularly useful in agricultural and environmental applications due to their semiconducting nature[14], photocatalytic, antibacterial properties and use as a fertilizer.[15–17] Various physicochemical methods, such as mechanochemical[18], polyol[19], solvothermal[20], hydrothermal[21], and thermal decomposition[22], have been used for the synthesis of ZnO-NPs. Although these are effective methods for preparing nanoparticles with different morphologies, shapes, and ecotoxicities, they require toxic reducing agents and high-energy fabrication. In contrast, biological methods use microorganisms such as *Serratia nematodiphila*[23], *Bacillus foraminis*[24], *Lactococcus lactis*[25], *Cordyceps militaris*[26], and plants like *Ziziphus spina-christi*[27], *Thymbra Spicata*[28], *Capparis spinosa*[29], *Moringa oleifera*[30], and *Allium saralicum*[31] for the fabrication of ZnO-

View Article Online
DOI: 10.1039/D6VA00120C

NPs. Microbial-based fabrication of NPs is environmentally friendly, but the synthesis rate is low, making large-scale production difficult. However, plant-based synthesis can overcome the issues of the physiochemical and microbial fabrication of nanoparticles due to a fast production rate, limited use of toxic chemicals and stabilizing agents such as phenolics, flavonoids, and alkaloids[4] for the synthesis of ZnO-NPs.

Agriculture systems which are being irrigated with textile effluent pose a significant threat to the security of food. Mung beans, termed *Vigna radiata* are leguminous, nutrient-rich crop whose yield and production are affected by textile wastewater in countries such as Pakistan. Kothari et al.[32] reported a study on the germination and growth of *Vigna radiata* under heavy metals and dyes stress, present in the textile wastewater. Genotoxic and cytotoxic contaminants of textile effluent decreased the mitotic index, enhanced chromosomal abnormalities and affected plant health.[33] Previously, different microbial species, including *Citrobacter*[34] and *Bacillus*[35] have been used to overcome the phytotoxicity of textile effluents. In addition, iron oxide nanoparticles[4] and titanium oxide nanoparticles[36] have also been reported recently. Numerous nanomaterials have been tested for wastewater treatment and better plant growth, but limited data is available on the textile wastewater along with ZnO-NPs, on the germination and growth of Mung bean. The present study was designed to synthesize efficient and sustainable nanomaterials for the treatment of textile effluents with better agricultural yield and productivity under wastewater stress. Firstly, the ZnO-NPs were synthesized chemically using NaOH and biologically using *Conocarpus erectus* leaves for synthetic and actual textile wastewater treatment. Furthermore, this study optimized the threshold dosage of synthesized materials by evaluating their influence on the germination of Mung beans. Finally, the optimum dosage of ZnO-NPs was determined, suggesting their effective application in alleviating wastewater-induced phytotoxicity in *Vigna radiata*.

2. Material and methods

View Article Online
DOI: 10.1039/D6VA00120C

2.1 Materials and chemicals

Fresh leaves of *Conocarpus erectus* were obtained from the botanical garden of the Government College University, Faisalabad, Pakistan. All chemicals and reagents, including zinc sulfate heptahydrate, sodium hydroxide, sodium borohydride, acetone, and sulfuric acid, were of analytical grade and purchased from Sigma Aldrich.

2.1.1 Biosynthesis of ZnO-NPs

For the green synthesis of ZnO-NPs, the fresh leaves of *Conocarpus* were initially washed with tap water, subsequently with distilled water to remove dust particles, and then dried in an oven at 50 ℃. The dried leaves were ground into fine powder and used for extraction of their extract, following the method described in Batool et al.[4]. After the extract was obtained, 75 mL of 0.1 M solution of $ZnSO_4$. $7H_2O$ was prepared and mixed with 25 mL of extract with continuous stirring for around 3 hours on a hot plate. This reaction mixture was sonicated for 30 minutes and centrifuged (10 minutes at 7000 rpm) to remove the supernatant. The NPs pellet was rinsed with deionized water to remove any surface impurities, dried in an air oven and ground into fine powder with the aid of ceramic mortar and pestle. The proposed mechanism behind the *Conocarpus* based synthesis of NPs is shown in **Fig. 1**.

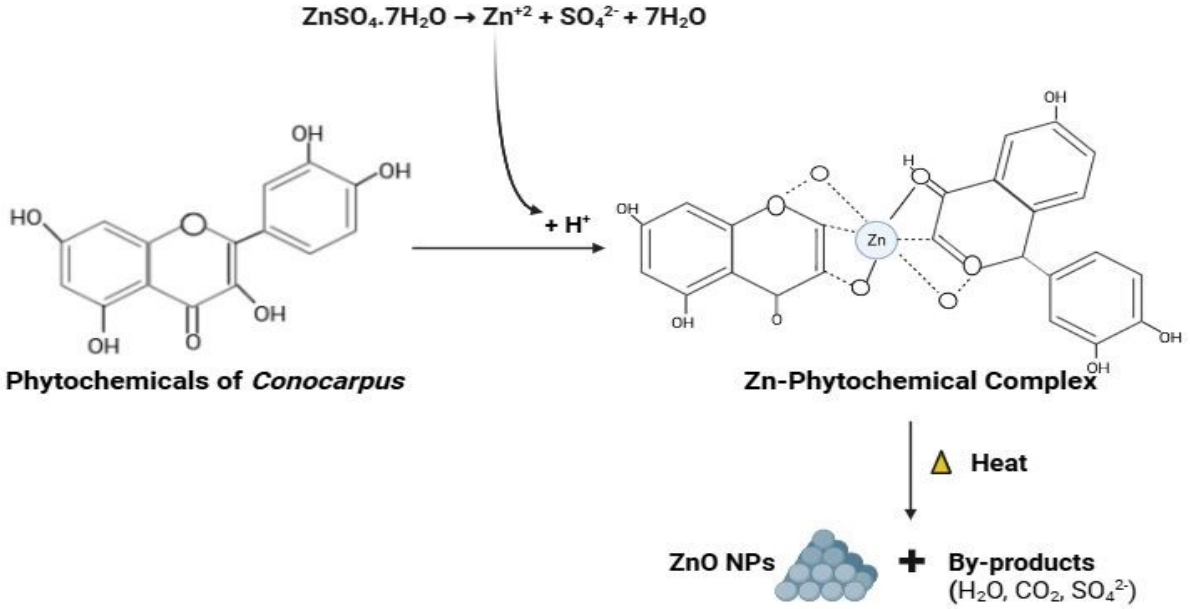

View Article Online
DOI: 10.1039/D6VA00120C

Fig. 1 Schematic mechanisms of biosynthesis of ZnO-NPs using leaf extract of *Conocarpus erectus*

2.1.2 Chemical synthesis of ZnO-NPs

For chemical production of ZnO-NPs, a 0.25 M solution of $ZnSO_4$. $7H_2O$ was prepared (Equation 1) and slowly hydrolyzed with 0.25 M solution of NaOH (Equation 2 and 3) with continuous stirring for around 24 hours. This reaction mixture was sonicated for 30 minutes and centrifuged (10 minutes at 7000 rpm) to remove the supernatant. The NPs pellet was rinsed with deionized water to remove any unreacted residuals, dried in an air oven, and ground into fine powder with the aid of ceramic mortar and pestle.

$$ZnSO_4.7H_2O \rightarrow Zn^{2+} + SO_4^{2-} + 7H_2O \ldots (1)$$

$$Zn^{2+} + 2NaOH \rightarrow Zn(OH)_2\downarrow + 2Na^{+} \ldots (2)$$

$$Zn(OH)_2 \xrightarrow{\Delta} ZnO + H_2O \ldots (3)$$

2.1.3 Characterization of ZnO-NPs

The synthesized ZnO nanomaterials were analyzed using different characterization techniques. Ultraviolet visible spectrophotometer was used to confirm the synthesis of ZnO-NPs. After confirmation, the synthesized nanomaterials were subjected to Scanning electron microscopy (SEM) for estimation of their shape. The determination of functional groups on the surface of ZnO-NPs was confirmed through Fourier Transform Infrared (FTIR) Spectrophotometer. Finally, the size and crystalline nature of the NPs were confirmed by X-ray diffraction (XRD) analysis.

2.2 Application of ZnO-NPs for the treatment of dyes-laden synthetic wastewater

The bio and chemically synthesized ZnO-NPs were used for the decolorization of five dyes namely methylene blue (MB), congo red (CR), reactive black-5 (RB-5), malachite green (MG), and reactive red-2 (RR-2) from the synthetic water under different conditions. The proposed mechanism for the decolorization of the dye is shown in **Fig. 2**.

View Article Online
DOI: 10.1039/D6VA00120C

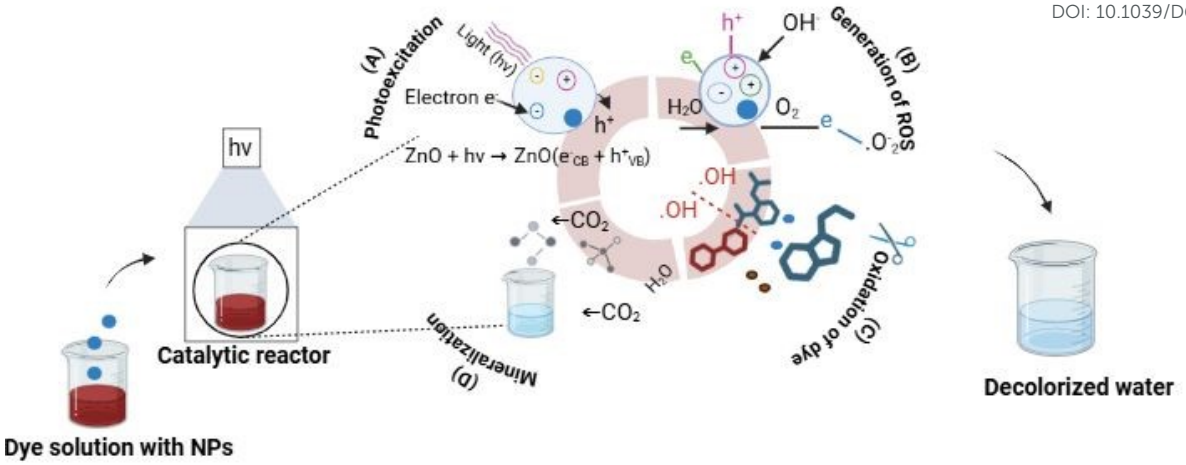

Fig. 2 Schematic mechanisms behind the decolorization of dyes using ZnO-NPs

2.2.1 Optimization of ZnO-NPs for the decolorization of Congo red dye

The synthesized ZnO-NPs were initially optimized for the removal of congo red dye. Different concentrations of NPs like 0.5, 1, 1.5, and 2 mg mL^{-1} were added to the dye solution having 50 ppm concentration and placed under sun incubation with uninoculated control. This experiment was performed in triplicates (n=3). About 2 mL sample were taken from each reaction mixture and subjected to spectrophotometer for the estimation of optimum concentration of NPs, after specific time interval. The % dye decolorization was calculated using the formulae described in equation 4,

$$\text{Dye decolorization (\%)} = (C\text{-}S/C) \times 100 \ldots (4)$$

The optimized concentrations of nanomaterials were further used for the treatment of synthetic wastewater under different conditions. However, their experimental details and results have been added to supplementary information (Section S.1-S.2).

2.3 Application of ZnO-NPs for the treatment of actual wastewater

The potential of optimized dosage of ZnO-NPs was additionally estimated for real textile wastewater treatment. The wastewater samples were obtained from the drainage namely Paharang drain, Samundri (N-31.398127 and E-73.079553) and Sargodha (N-31.526904 and E-73.118483) roads, Pakistan. The wastewater samples were mixed and filtered initially to

View Article Online
DOI: 10.1039/D6VA00120C

separate the suspended particles. After filtration, the filtrate was enriched with CR dye to have considerable dye concentration and color intensity. The dye was also added to ensure the consistent spectrophotometric evaluation of dye removing potential of prepared ZnO-NPs while maintaining the other physicochemical properties of textile wastewater. The optimized concentrations of bio and chemically synthesized ZnO-NPs were added to the dye laden wastewater sample (n=3) keeping the untreated control sample independent, for wastewater treatment. The reaction solution was shaken for an hour and different parameters like, pH, color intensity, electrical conductivity (EC), Cr-reduction, chemical oxygen demand (COD), total dissolved solids (TDS), Phosphate, and Sulphate were estimated before and after the treatment.

2.4 Optimization of ZnO-NPs for the growth of Mung bean (*Vigna radiata)*

After the treatment of textile wastewater, different concentrations (0, 25, 50, 75, and 100 mg L^{-1}) of ZnO-NPs were applied to *Vigna radiata* for evaluating their threshold level. This experiment was conducted in petri plates (n=3). About 13 seeds were added to each petri plate and treatments were applied on alternative days for 7 days. Different parameters, such as total germination (G%), chlorophyll content, superoxide dismutase (SOD), and hydrogen peroxide (H_2O_2), were considered for the selection of optimum dosage of bio and chemically synthesized ZnO-NPs following the protocol described in Batool et al. [37] and Shafqat et al. [38].

2.5 Effect of Optimized Dosage of ZnO-NPs on Germination of *Vigna Radiata* (mung bean) Under Textile Wastewater Stress

After evaluating the threshold of ZnO-NPs, the effect of optimum dose of ZnO-NPs (bio and chemically synthesized) along with treated and untreated effluent on the seed germination of mung bean was studied. The complete randomized experiment (n=3) was again conducted in petri plates in a growth chamber having temperature between 26-28 ℃ and Light of about 16/8 hours. Around 13 seeds were put into each petri plate after dipping in D. H_2O and wastewater. All the selected treatments (T) were foliarly applied on intermittently days, and the treatment

View Article Online
DOI: 10.1039/D6VA00120C

layout is presented in **Table 1**. The germinated seeds were counted daily, and the collected data were used to estimate different seed germination parameters, such as time to 50 % germination (50% G), germination % (G%), mean emergence time (MET), coefficient of uniformity of emergence (CUE), emergence index (EI), and length using the protocol described in Batool et al. [4].

Table 1. Treatment layout designed for the growth and germination of mung bean (*Vigna radiata)* under wastewater stress

Treatments	**Description**
T1	Positive control (D. H_2O)
T2	D. H_2O + ZnO(C)-NPs
T3	D. H_2O + ZnO(B)-NPs
T4	Negative control (Wastewater (WW))
T5	WW + ZnO(C)-NPs
T6	WW + ZnO(B)-NPs
T7	Treated wastewater (TWW) using ZnO(C)-NPs
T8	TWW using ZnO(B)-NPs
T9	TWW using ZnO(C)-NPs + ZnO(C)-NPs
T10	TWW using ZnO(B)-NPs + ZnO(B)-NPs

2.6 Estimating the effect of optimized dosage of synthesized nanomaterials and treated effluent on growth of *Vigna radiata* under stress

2.6.1 Experimental detail

The pot experiment was conducted in a growth chamber having temperature of about 26-28 ℃ and light of 16/8 hours in Government College University Faisalabad. The seeds (10 seeds per pot) of *Vigna radiata* were procured from the Ayub Agriculture Research Institute, Pakistan. The sandy loam textured soil was also collected from the research institute having organic

View Article Online
DOI: 10.1039/D6VA00120C

content of 0.87, EC of 2.59, potassium of 159, phosphorous of 11.9, and nitrogen of 0.71. The experiment was arranged in complete random design (CRD) with three replicates (Total number of pots=30) of each treatment. All the designed treatments (**Table 1**) were applied intermittently for 21 days. After harvesting, the *Vigna radiata* seedlings were tested for growth (root length RL, shoot length SL, root weight RW and shoot weight SW), photosynthetic (Chlorophyll a, b, total chlorphyll, and carotenoids), enzymatic antioxidants (catalase CAT, peroxidase POD, and superoxide dismutase SOD), and oxidative stress (malondialdehyde MDA, and hydrogen peroxide H_2O_2) attributes.

2.7 Statistical analysis

All results were analyzed statistically using Statistix 8.1 software, and graphs were created using GraphPad Prism 8. One-way ANOVA was applied to examine the difference between the treatments and post hoc test (LSD) was utilized for the comparisons of means. The difference between the applied treatments were considered statistically significant at $p \leq 0.05$. For multivariant analysis, R-studio (4.2.2) was used to make heat maps and principal component analysis PCA.

3. Results and discussions

3.1 Synthesis and characterization of bio and chemically synthesized ZnO-NPs

The *Conocarpus* and NaOH derived ZnO-NPs were synthesized and characterized for the determination of their structure, crystalline nature, and presence of different functional groups. During synthesis, the addition of precursor salt solution to the plant extract and NaOH, the reaction mixture color was changed from yellowish to pale brown and transparent to milky as shown in **Fig. S4**. This was the first confirmation of the production of ZnO(B)-NPs and ZnO(C)-NPs. The UV-vis spectrum of ZnO(B)-NPs and ZnO(C)-NPs showed an absorption peak at 398 (**Fig. 3A**) and 352 nm (**Fig. 3B**), respectively. In contrast Ogunyemi et al.[39] synthesized ZnO-NPs using leaf extract of *Matricaria chamomilla* L., *Olea europaea*, and

View Article Online
DOI: 10.1039/D5VA00120C

*Lycopersicon esculentum*s and observed their peaks at 384, 380, and 386 nm, respectively. They also reported that the phytochemicals such as flavonoids, glycosides, and tannins are responsible for the reduction of zinc salt into nanoparticles. The spectrum of FT-IR confirmed the presence of distinct functional groups on the surface of ZnO-NPs. The transmittance peak (**Fig. 3C**) at 3527.9 cm^{-1} was due to the presence of the OH group, while the peak at 2925.3 cm^{-1} was due to the stretching of the C-H bond. Phosphines of C=C and C≡C primary amine groups were observed at 2400.7 and 2150.0 cm^{-1}. The peaks at 1698 and 1151.7 cm^{-1} were due to the presence of C=O and C-F groups. The alkyl amine and C-O-H bonds were observed at 1104.7 and 1050.2 cm^{-1}. The peak at 1000.8 cm^{-1} was due to the C-F and 935 cm^{-1} was due to ZnO stretches. On the other hand, the FT-IR spectrum of ZnO(C)-NPs (**Fig. 3D**) showed peaks at 3361 and 2890 cm^{-1}, which were due to N-H and C-H bonds. The peaks at 2370.2 and 2195 cm^{-1} confirmed the presence of the C≡N and C≡C bonds. The CH_2 bending was noted at 1430 cm^{-1}. The peaks at 1104 and 805 cm^{-1} belongs to alkyl amide and C-Cl groups. Datta et al.[40] observed the peaks of ZnO-NPs at 3458, 2451, 2270, 2245, 1643 and 424 cm^{-1} that were assigned to OH, C≡N, and C≡C groups. The FTIR spectrum confirmed that enzymes present in extract are responsible for the stability, reduction and capping of nanomaterials. Meanwhile, the XRD pattern of the ZnO-NPs displayed characteristic diffraction peaks and confirmed the hexagonal wurtzite phase of NPs, including prominent reflections at 2θ values of approximately 31.8°, 34.4°, and 36.2° (**Fig. 3E and 3F**), indexed to the (100), (002), and (101) planes, respectively. The results of XRD analysis are consistent with the findings of Stan et al.[41], they also confirmed the hexagonal wurtzite structure of ZnO-NPs. However, the peaks of ZnO(B)-NPs were relatively broader and less intense, indicating a smaller crystallite size and lower crystallinity, which can be attributed to the presence of bio-organic compounds during synthesis. In contrast, the chemically synthesized ZnO-NPs exhibited sharp and well-defined peaks at the same 2θ positions, confirming the formation of a highly crystalline, phase-pure

View Article Online
DOI: 10.1039/D6VA00120C

ZnO structure. Finally, the SEM images of ZnO-NPs (**Fig. 3G and 3H**) revealed irregular, aggregated particles with a rough and blocky morphology.

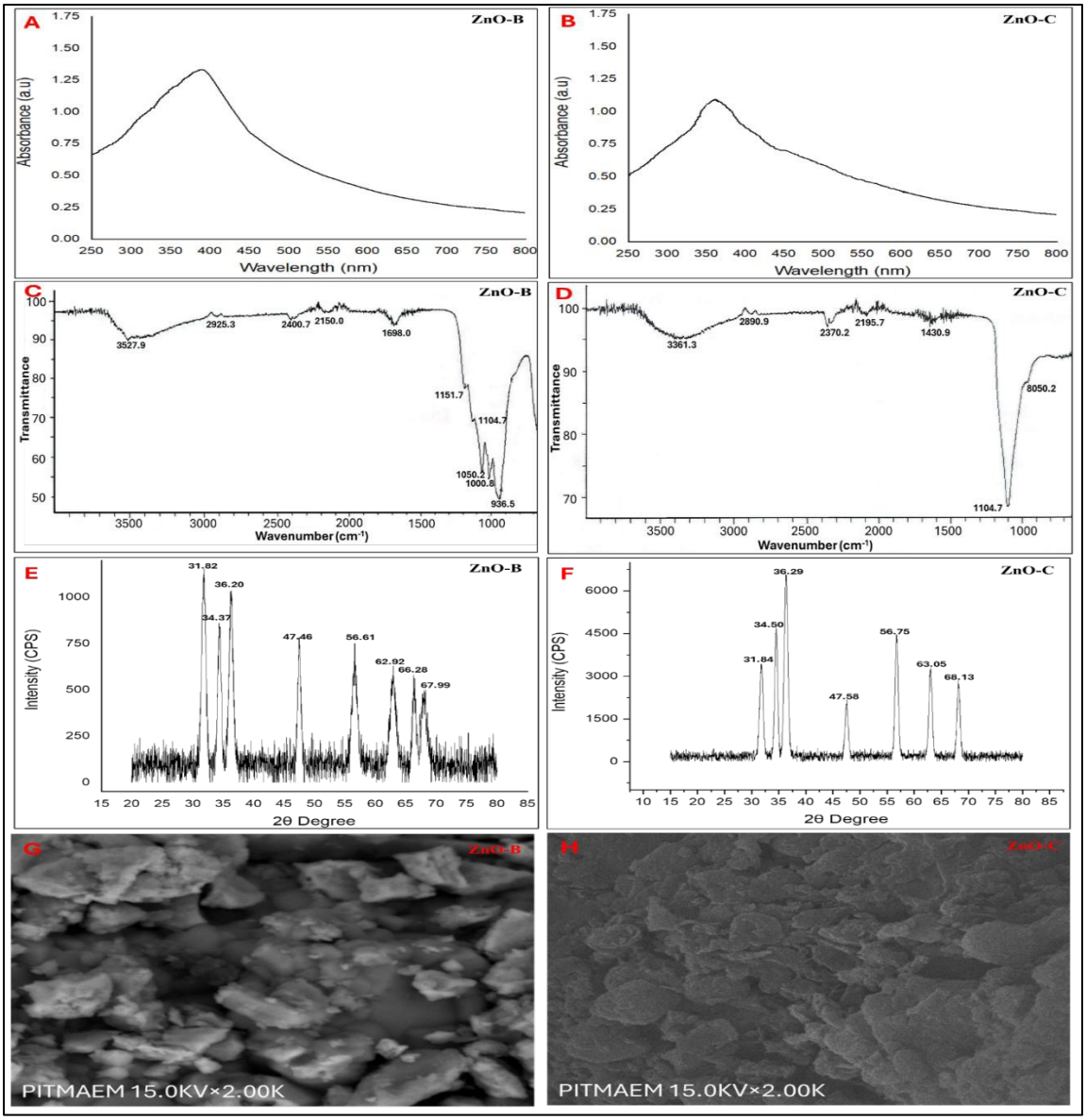

Fig. 3 Characterization of bio (UV-Vis (A), FTIR (C), XRD (E), SEM (G)) and chemically (UV-Vis (B), FTIR (D), XRD (F, SEM (H)) synthesized ZnO-NPs

3.2 Application of ZnO-NPs for the treatment of synthetic wastewater

3.2.1 Optimization of ZnO-NPs for the decolorization of Congo red dye

The decolorization potential of ZnO(C)-NPs and ZnO(B)-NPs was studied using four different concentrations under solar irradiation of about 4 hours (**Fig. 4**). The decolorization efficiency

View Article Online
DOI: 10.1039/D6VA00120C

of ZnO-NPs increased with time and concentration. It was found that at 0.5 mg mL^{-1} the efficiency of ZnO(C)-NPs (**Fig. 4A**) increased from 13.88 ± 0.64% after 1 hour to 36.34 ± 1.24% after 4 hours. The higher concentrations resulted in more decolorization with 87.99 ± 3.06% at 2.0 mg mL^{-1} after 4 hours of solar incubation. A parallel trend was observed at 1.0 and 1.5 mg mL^{-1}, suggesting that ZnO(C)-NPs require a higher dosage to reach optimal performance. The results for ZnO(C)-NPs are aligned with those of Ahmed et al.[42] They described that the decolorization potential of ZnO-NPs increased with increasing catalyst concentrations. It might be due to the increasing number of active sites present on the surface of nanoparticles, which generate more photogenerated holes and hydroxyl radicals for the degradation of dyes.[43] Conversely, ZnO(B)-NPs exhibited the highest decolorization efficiency at the lowest concentration of 0.5 mg mL^{-1}, achieving 80.41 ± 1.95% after 4 hours (**Fig. 4B**). Although 1.0, 1.5, and 2.0 mg mL^{-1} also showed considerable dye removal, their potential remained slightly lower than that of 0.5 mg mL^{-1}. The observed trend might be attributed to the aggregation of nanomaterials as reported by [44], which may reduce the surface area available for the attachment of dye molecules.[45] It reduces the absorption of photons and the production of reactive oxygen species like superoxide anions and hydroxyl radicals required for the degradation of dyes.[40,42,43] These results support the better performance of ZnO(B)-NPs at 0.5 mg mL^{-1} and for ZnO(C)-NPs, it was 2.0 mg mL^{-1}, respectively.

Meanwhile, the cluster heatmap analysis was carried out to identify the most effective and optimum concentration of ZnO-NPs for decoloring dyes from synthetic wastewater. It (**Fig. 4C**) shows the clustering of nanoparticles (Y Axis) over distinct time intervals and concentrations (X Axis). In this analysis, dark green color indicates higher activity, and light colors suggest lower decolorization potential. The results confirmed that ZnO(C)-NPs showed maximum decolorization at a concentration of 2.0 mg mL^{-1} and ZnO(B)-NPs displayed optimal decolorization at 0.5 mg mL^{-1} especially after 4 hours. Additionally, principal component

View Article Online
DOI: 10.1039/D6VA00120C

analysis (PCA) was carried out to evaluate the effect of each concentration of ZnO(B)-NPs and ZnO(C)-NPs on the decolorization of CR (**Fig. 4D**). In database, DIM 1 and DIM 2 showed 99.8% contribution (DIM 1 contributed 97.9 % and DIM 2 contributed about 1.9%). The analysis revealed that different nanomaterial concentrations significantly affected CR dye decolorization.

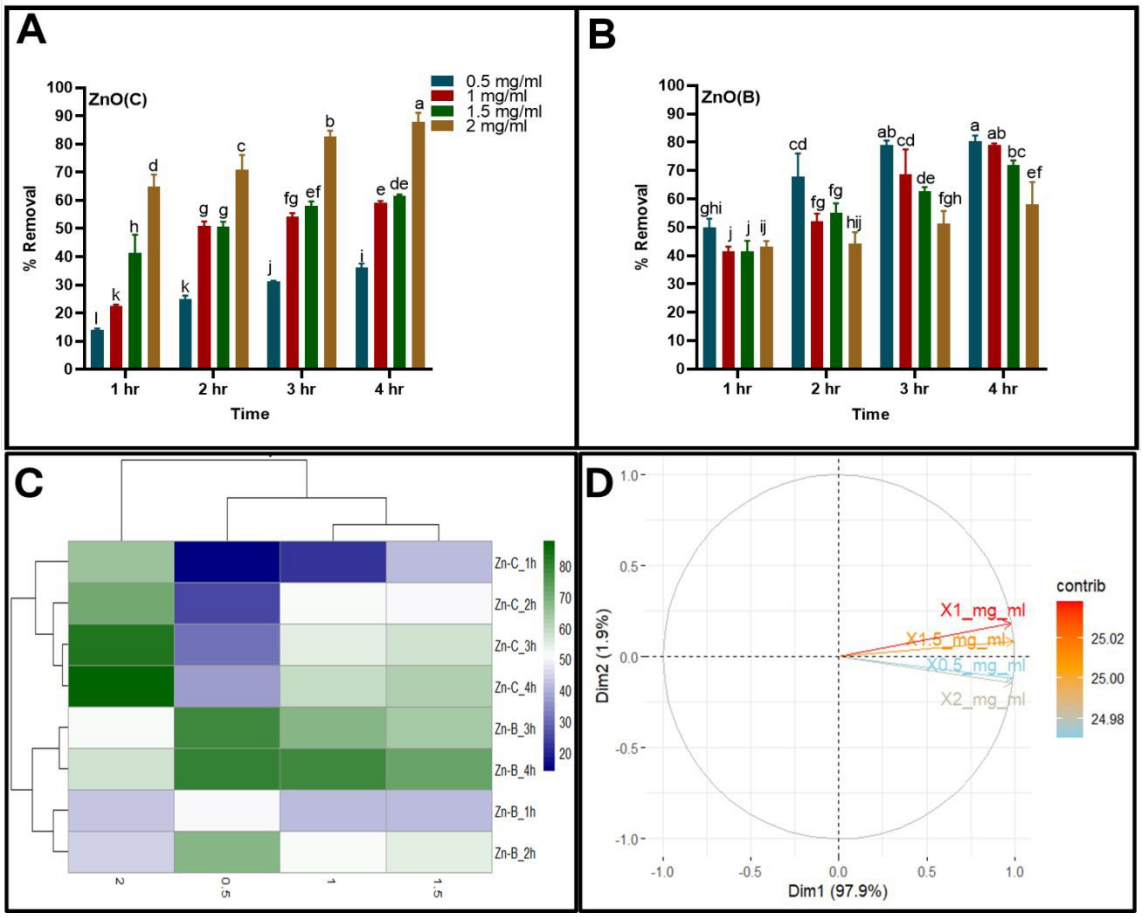

Fig. 4. Removal of Congo red (CR) dye using multiple concentrations (0.5, 1, 1.5, and 2 mg mL^{-1}) of bio and chemically prepared ZnO-NPs. Bar graphs represent the decolorization of dyes while PCA and heat map demonstrate the multivariant analysis. Error bars represent the standard deviation (n=3)

3.3 Application of ZnO-NPs for the treatment of actual wastewater

After synthetic wastewater treatment, the bio-and chemically synthesized ZnO-NPs were used to treat the actual wastewater of textile industries (**Table 2**). The visual representation of

View Article Online
DOI: 10.1039/D6VA00120C

wastewater treatment is shown in **Fig. 5A**. It was observed that untreated wastewater was characterized with high pH (9.01±0.05), EC (4036±7.25), TDS (2650±10), color intensity (0.432±0.01), sulphate (757.1±9.38), phosphate (27.69±0.30), and COD (124.71±1.39) levels. The application of ZnO(B)-NPs improved the quality of wastewater significantly by reducing tested parameters. It lowers the pH of effluent to 7.85±0.06 while ZnO(C)-NPs reduced it to 8.17±0.04, compared to untreated wastewater. The EC of effluent was reduced to 3416±5.29 by ZnO(B)-NPs and 3980±9.01 by ZnO(C)-NPs. Additionally, the remediation of textile wastewater with ZnO(B)-NPs lowered the color intensity, sulfate, phosphate, and COD by 72.58%, 43.54%, 79.37%, and 71.30%, respectively. Conversely ZnO(C)-NPs reduced the color intensity by 67.28%, sulphate by 15.75%, phosphate by 60.88%, and COD by 46.58%, compared to wastewater. The reduction in color intensity is due to the production of ROS (reactive oxygen species) as discussed earlier while the decrease in pH, TDS, COD, and EC might be due to the oxidation and photo-transformation of pollutants initiated by the production of oxidizing species after absorbing sunlight at surface of ZnO-NPs.[4, 48] The decrease in phosphate and sulphate contents is may be because of the precipitation process, started by solar light.[49]

During multivariant analysis, the heat map (**Fig. 5B**) clearly demonstrated the presence of high level of pollutants in untreated wastewater (control), indicated by blue color. The biosynthesized ZnO-NPs treated the wastewater more efficiently as compared to ZnO(C)-NPs as shown by red color (positive relationship). The PCA of parameters (**Fig. 5C**) showed that most of the parameters were strongly correlated and contributed to DIM-1, which accounted for 92.3% of the total variance. In contrast, DIM-2 accounted for 7.7% of the variance. The PCA of treatments (**Fig. 5D**) additionally confirmed that ZnO(B)-NPs have superior potential of treating effluent by positioning on positive side of DIM-1 and ZnO(C)-NPs have partial potential confirmed by intermediate positioning.

View Article Online
DOI: 10.1039/D6VA00120C

Table 2 Treatment of real textile wastewater with ZnO(B)-NPs and ZnO(C)-NPs

Treatments	Variables						
	pH	Electrical conductivity (µS cm^{-1})	Total dissolved solids (mg L^{-1})	Color intensity (abs)	Sulphate (mg L^{-1})	Phosphate (mg L^{-1})	Chemical oxygen demand (mg L^{-1})
Control	9.01±0.05	4036±7.25	2650±10	0.434±0.01	757.16±9.38	27.69±0.30	124.71±1.29
ZnO(B)-NPs	7.85±0.06	3416±5.29	1894±3.60	0.119±0.003	427.44±3.93	5.71±0.10	35.785±1.85
% Removal	-	-	28.52	72.58	43.54	79.37	71.30
ZnO(C)-NPs	8.17±0.04	3980±9.01	2090±4	0.142±0.01	637.86±9.44	10.83±0.37	66.619±2.77
% Removal	-	-	21.13	67.28	15.75	60.88	46.58

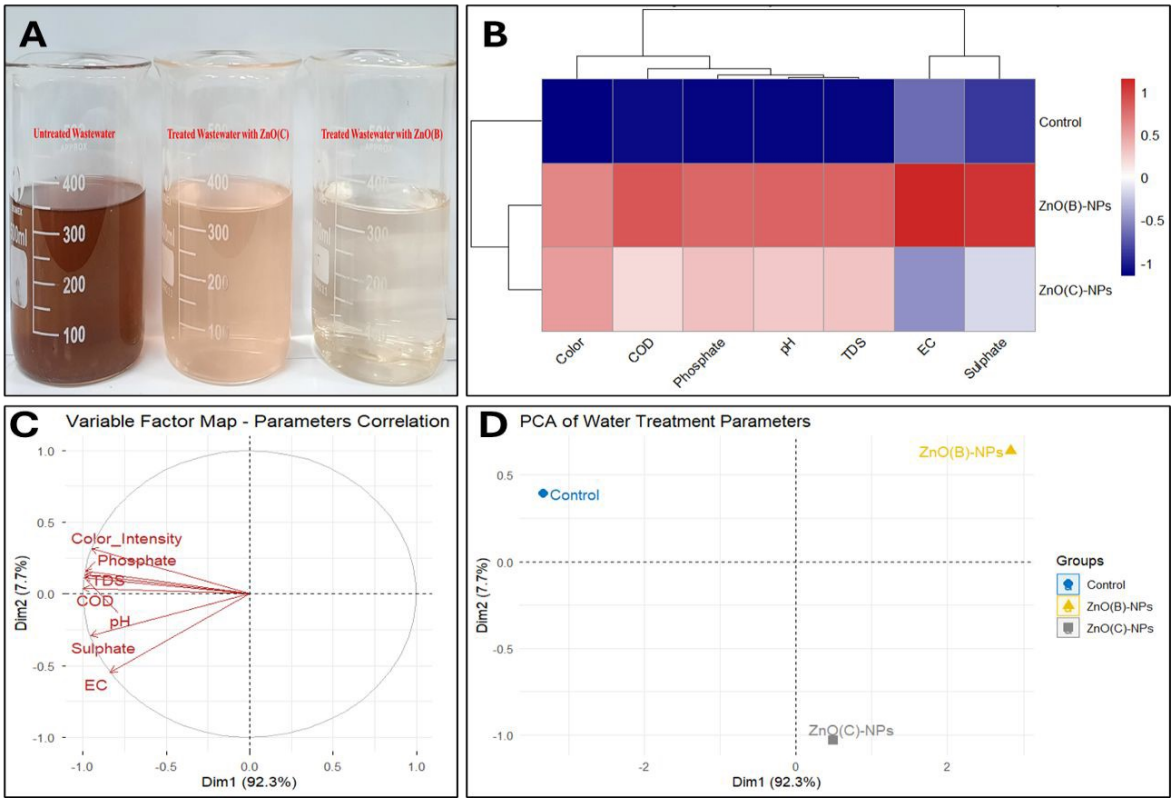

Fig. 5 Multivariant analysis of wastewater treatment using bio and chemically synthesized ZnO-NPs

View Article Online
DOI: 10.1039/D6VA00120C

3.4 Optimization of ZnO-NPs for the growth of *Vigna radiata*

After textile wastewater treatment, different concentrations of bio and chemically prepared ZnO-NPs were used to evaluate their threshold level for the growth of *Vigna radiata*. It was noticed that highest germination was seen at 75 mg L^{-1} and 100 mg L^{-1} of ZnO(B)-NPs followed by 50 mg L^{-1}, and 25 mg L^{-1} **(Table 3).** Conversely the application of chemically synthesized counterparts showed the maximum germination at 50 and 75 mg L^{-1}. Similarly, the maximum total chlorophyll content was observed at 100 mg L^{-1} by ZnO(B)-NPs and 50 mg L^{-1} by ZnO(C)-NPs. Briefly, it was noticed that the chlorophyll content was increased in *Vigna radiata* with the increase in concentration of ZnO(B)-NPs, but the application of ZnO(C)-NPs increased the chlorophyll content till 50 mg L^{-1}, further increase of NPs induced the phytotoxicity. Additionally, the H_2O_2 content was also estimated, and it was observed that minimum oxidative stress was observed at 75 and 50 mg L^{-1} of ZnO(B)-NPs and 50 mg L^{-1} of chemically synthesized nanomaterials. The maximum antioxidative stress (SOD) was observed at 100 mg L^{-1} of ZnO(B)-NPs and 50 mg L^{-1} of ZnO(C)-NPs. The findings of the study are in consistent with the results of Shafqat et al. [38] They applied different concentrations of ZnO-NPs on cotton and reported that 100 ppm of biosynthesized nanomaterials was the optimal dosage for the growth of crops. The difference in optimal dosages of bio and chemically synthesized nanomaterials might be due to the selection of reducing agents. The toxicity of chemically synthesized NPs at high concentrations may lead to the displacement of magnesium ions in the chlorophyll molecules and inhibition of enzymes, such as aminolaevulinic acid dehydratase (ALAD), leading to chlorosis. Conversely, the higher threshold of ZnO(B)-NPs may be due to the natural capping agents which may slowly release the zinc ions and prevent the chloroplast membrane from being disrupted by the sudden influx of ions.[50] The findings of this experiment were further confirmed using multivariate analysis. The heat map in **Fig. 6A** shows a clear difference in the applied treatments, where ZnO(B)-NPs cluster together at 75

View Article Online
DOI: 10.1039/D6VA00120C

and 100 mg L^{-1} and show a positive relationship (red color) for all tested parameters. Meanwhile the highest concentration of ZnO(C)-NPs showed negative relationship (blue color), affecting physiological parameters and elevating stress. The PCA of the parameters (**Fig. 6B**) also confirmed this trend, where germination, chlorophyll content, and SOD load followed a positive direction along DIM-1 (81.8% of the total variance), whereas the hydrogen peroxide was negatively correlated, indicating it as a stress indicator. Meanwhile the PCA of treatments (**Fig. 6C**) confirmed that application of ZnO(B)-NPs showed a strong and consistent positive physiological response. Therefore, 100 mg L^{-1} ZnO(B)-NPs and 50 mg L^{-1} ZnO(C)-NPs were determined as the optimal dosages for the efficient growth of *Vigna radiata.*

Table 3 Impact of multiple concentrations of bio and chemically synthesized ZnO-NPs on growth of *Vigna radiata*

	0 mg L^{-1}	**25 mg L^{-1}**		**50 mg L^{-1}**		**75 mg L^{-1}**		**100 mg L^{-1}**	
Parameters	**Distilled water**	**ZnO(B)-NPs**	**ZnO(C)-NPs**	**ZnO(B)-NPs**	**ZnO(C)-NPs**	**ZnO(B)-NPs**	**ZnO(C)-NPs**	**ZnO(B)-NPs**	**ZnO(C)-NPs**
Total germination	9±3	10±2	9±1	11±1	12±3	13±2	12±3	13±1	9±2
Total Chlorophyll (mg g^{-1})	2.1±0.006	3.19±0.035	2.96±0.07	3.47±0.05	3.59±0.04	3.81±0.008	2.11±0.01	4.01±0.07	1.37±0.03
Hydrogen peroxide (nmolg^{-1}FW)	10.7±0.1	18.77±0.43	15.01±0.09	10.46±0.28	9.11±0.81	6.84±0.73	18.29±0.69	6.80±0.61	27.38±0.79
Superoxide dismutase (mg^{-1} protein)	30.0±0.02	29.51±0.06	24.62±0.82	35.32±0.49	31.52±0.21	43.11±0.36	26.39±0.04	47.18±0.18	19.98±0.02

View Article Online
DOI: 10.1039/D6VA00120C

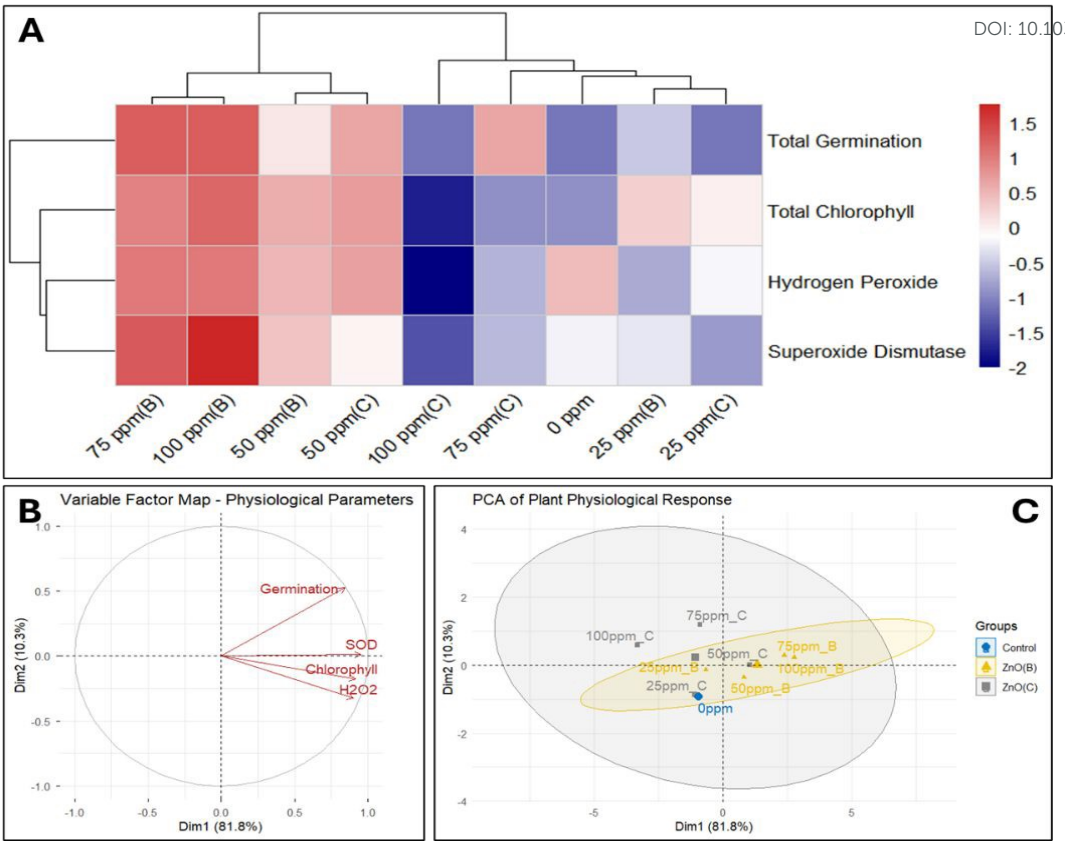

Fig. 6 Multivariant analysis showing the impact of multiple concentrations of biologically and chemically prepared ZnO-NPs on growth and biochemical attributes of *Vigna radiata*

3.5 Effect of optimized dosage of ZnO-NPs on seed germination (SG) of *Vigna radiata* under wastewater stress

After evaluating the threshold of biologically and chemically synthesized ZnO-NPs, the optimum dosage of each nanomaterial was used to study their effect on the germination of mung bean under wastewater stress (**Fig. 7**). It was monitored that T3 application decreased days to 50% G by 65% in contrast to positive control (distilled water application T1), while the T2 application improved the days to 50% G by 26% (**Fig. 7A**). This improvement in germination by ZnO-NPs might be due to the fact that zinc is a vital component of seed metabolism, especially in the activation of hydrolytic enzymes like alpha- amylase, which may increases the mobilization of seed reserves and fast prominence of the radicle.[51] The wastewater (T4) application significantly enhanced the time of 50% G as compared to the

View Article Online
DOI: 10.1039/D6VA00120C

positive control (T1), which might be due to the presence of dyes, heavy metals, and other organic pollutants that induce phytotoxicity. However, the synthesized ZnO-NPs with different treatments reduced the time of 50% G under effluent stress. The applications of T6, T8, and T10 decreased in the days to 50% G by 54%, 58%, and 77% as compared to the wastewater (T4) application. Whereas the applications of T5, T7, and T9 decreased the effect of effluent by decreasing the days to 50% G by 48%, 56%, and 61%. The G% was also calculated and it was observed that maximum germination appeared in the application of T3, and the minimum germination was noticed in wastewater (negative control T4) application (**Fig. 7B**). However, T5-T10 applications significantly decreased their impact by increasing the germination %. In case of mean emergence time, the application of T2 increased it by 14% but the ZnO(B)-NPs (T3) decreased the MET by 27.4% in comparison to positive control (T1) (**Fig. 7C**). The application of ZnO-NPs (T5-T10) decreased the impact of effluent and significantly reduced the MET as compared to T4. Meanwhile, the emergence index was also calculated (**Fig. 7D),** and it was noticed that highest EI was observed in the application of T3, and least EI was observed in the application of wastewater. The T5-T10 applications lowered the wastewater (T4) impact by increasing EI, especially the application of green synthesized NPs outperformed the chemically synthesized counterpart by showing high EI. This improvement in the observed parameters under stress may be due to natural phytochemical capping, which improves the stability of nanoparticles, controls the release of Zn^{2+} as mentioned by Singh et al. [52], and strengthens the antioxidant defense mechanisms, thereby reducing oxidative damage and promoting uniform emergence.[53] Similar results were observed in case of CUE (**Fig. 7E**) and length (**Fig. 7F**).[54] The observed results were also confirmed by multivariant analysis. According to the PCA of the variables (**Fig. 7G**), all the observed parameters were clustered together and pointed towards the right side, showing a positive correlation between them. Meanwhile the PCA of treatment (**Fig. 7H**) showed that the control and treatments labelled as

View Article Online
DOI: 10.1039/D6VA00120C

T3, T8, T9, and T10 are clustered together and show prominent results. While T4 was positioned far to the left, it confirmed the negative impact of wastewater on the germination of *Vigna radiata.* From the heat map (**Fig. 7I**), it was clearly visualized that the application of T3 and T10 showed the most prominent results, as indicated by the red color (positive relationship). Conversely, wastewater induced phytotoxicity and showed a negative relationship (blue). Meanwhile, the application of T5 to T9 attempted to reduce the phytotoxicity of wastewater, as shown by the pink to dark red colors.

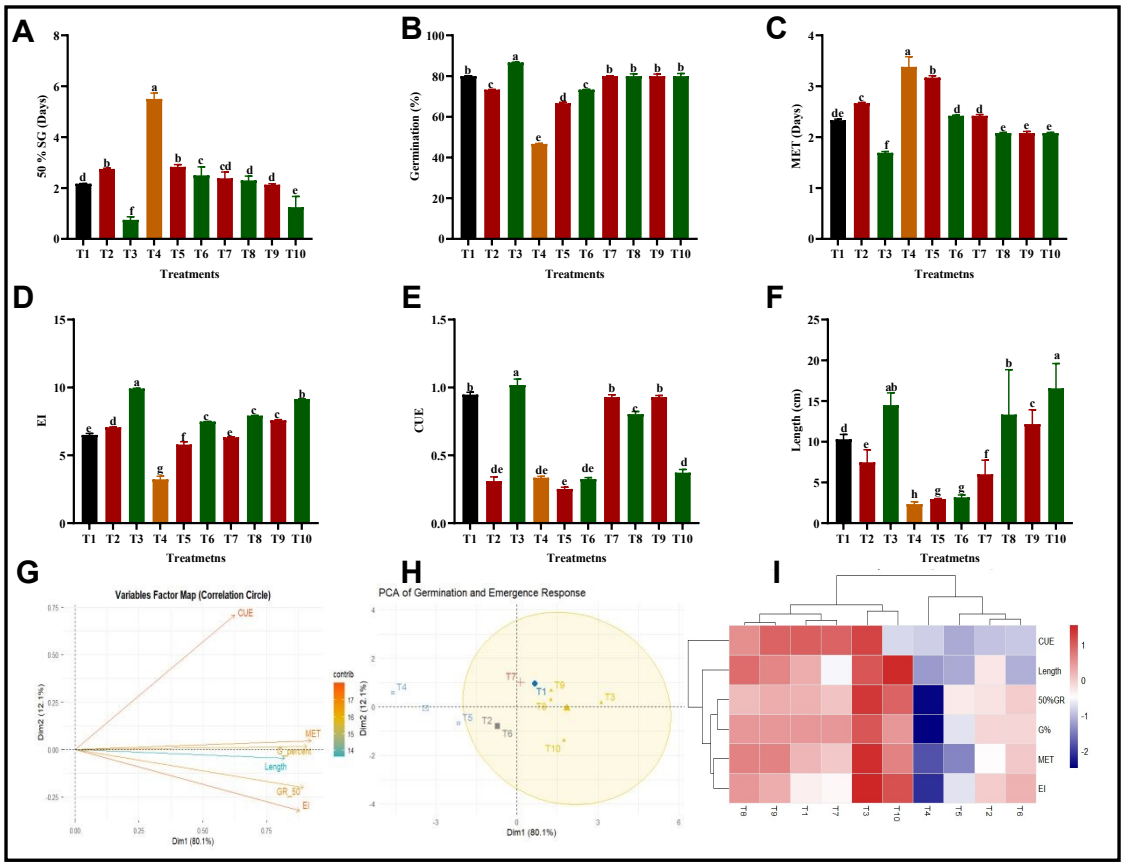

Fig. 7 Effect of different treatments on seed germination attributes of *Vigna radiata* under wastewater stress. Bar graphs represent the different germination parameters while PCA and heatmap demonstrate the multivariant analysis among treatment. Error bars represent the standard deviation (n=3) and distinct letters show significant differences among treatments

View Article Online
DOI: 10.1039/D6VA00120C

3.6 Estimating the effect of optimized dosage of synthesized nanomaterials and treated effluent on growth of *Vigna radiata* under stress

After evaluating the impact of synthesized nanomaterials and treated wastewater on germination, they were again foliarly applied to *Vigna radiata* grown in soil medium under stress of textile wastewater (**Fig. 8Q**). During the analysis of growth attributes, it was noticed that the application of ZnO(B)-NPs (T3) improved the RL **(Fig. 8A)**, SL **(Fig. 8B)**, RW **(Fig. 8C)**, SW **(Fig. 8D)** by 16.8%, 14.5%, 23.09%, and 28.98%, as compared to the application of distilled water (T1), whereas chemically synthesized ZnO-NPs increased them by 8.94%, 4.6%, 22.87%, and 7.39%, respectively. The wastewater (T4) application notably decreased the RL, SL, RW, SW by 49%, 26.0%, 65.33%. 73.1%, compared to the positive control (T1). However, T5 and T6 increased the RL by 31.7% and 37.3%, SL by 10.0% and 18.0%, RW by 52.2% and 54.9%, and SW by 44.4% and 65.2% as compared to the application of negative control (wastewater T4). The T7 and T8 applications further reduced the impact of wastewater by improving RL by 41.9% and 46.7%, SL by 21.7% and 25.2%, RW by 60% and 63.3%, and SW by 60.6% and 69.3%. The applications of T9 and T10 improved the RL by 45% and 52%, SL by 26% and 29%, RW by 67% and 73%, and SW by 68% and 75%, respectively as compared to the negative control (T4). Different studies have reported the impact of ZnO-NPs on enhancing crop growth under different stress conditions.[55–58] Mainly, Zinc is an essential micronutrient which is required for the synthesis and regulation of auxin.[57, 58] The sufficient availability of Zn may increase the division and elongation of cells, which improves shoot and root development, even under stress conditions.[61]

For photosynthetic content (Chl a, b, total chl, and carotenoid), it was noted that ZnO(B)-NPs increased the Chl a **(Fig. 8E)**, b **(Fig. 8F)**, total Chl **(Fig. 8G)**, and carotenoid **(Fig. 8H)** by 1.89%, 36.79%, 22.42%, and 9.75% relative to the application of distilled water (positive control). The application of wastewater reduced the photosynthetic content by reducing total

View Article Online
DOI: 10.1039/D6VA00120C

Chl and carotenoid by 56% in comparison to the application of distilled water (T1). However, T5 and T6 decreased the impact of wastewater by enhancing Chl a by 24.5% and 35.17), Chl b by 66.07% and 64.03%, total Chl by 48% and 50.03%, and carotenoid content by 31.91% and 36%, respectively. Similarly, T7 and T8 also lowered the phytotoxicity of textile effluent by increasing chlorophyll and carotenoid content in comparison to wastewater application (negative control). Meanwhile, nanomaterials application along with treated wastewater (T9 and T10) further decreased the impact by increasing Chl content by 60% and 63% and carotenoids by 33.3% and 60.49%, respectively. According to García-López et al.[62], ZnO-NPs increase the photosynthetic content in ionic form; it is the cofactor of several enzymes, mainly isomerase, ligase, transferase and hydrolase, which enhance the cellular performance when available in sufficient amounts. Meanwhile, Zinc is an important ion for osmoregulation, water relations, and mineral uptake. It can reduce ionic phytotoxicity, which ultimately increases the gaseous exchange in the affected plants.[63]

During the estimation of antioxidative attributes, it was noted that T3 application enhanced the CAT **(Fig. 8I)**, SOD **(Fig. 8J)**, and POD **(Fig. 8K)** by 0.52%, 16.6%, and 28.7% as compared to the application of distilled water (T1). Conversely, the application of wastewater significantly decreased CAT, SOD, and POD by 51.9%, 66.3%, and 71.14%, as compared to the positive control (T1). It might be due to the production and accumulation of reactive oxygen species which is responsible for the impairment of the antioxidative defense system.[64] The applications of T5 and T6 decreased the effect of wastewater by enhancing CAT, SOD, and POD by 21.3%, 57.8%, and 46.05%, respectively, compared to the application of wastewater. Additionally, T7 and T8 applications further decreased the impact of wastewater by increasing antioxidative stress parameters. Meanwhile, the application of T9 and T10 enhanced the CAT by 44% and 48.3%, SOD by 63.6% and 67%, and POD by 68.1% and 77%, respectively, under effluent stress. This improvement in the antioxidative stress system might be due to the reason

View Article Online
DOI: 10.1039/D6VA00120C

that ZnO-NPs may scavenge the ROS and help to maintain cellular redox balance. Briefly, the improvement in SOD activity may facilitate the conversion of superoxide radical into H_2O_2. In contrast, CAT and POD activities may further neutralize H_2O_2 and prevent oxidative damage in plants.[62, 63]

The impact of different treatments on oxidative stress parameters in *Vigna radiata* under wastewater stress was also investigated. The application of T3 decreased H_2O_2 **(Fig. 8L)** by 44.5% and MDA **(Fig. 8M)** by 83% compared to distilled water application (T1), whereas chemically synthesized counterparts decreased H_2O_2 by 23.7% and MDA by 74%. Conversely, the application of wastewater increased H_2O_2 and MDA levels by 53% and 67%, respectively, compared to the positive control (T1). This may be due to the production of ROS, which damages the cell membrane and increases lipid peroxidation.[37,66] The application of T5 and T6 reduced the impact of effluent by reducing H_2O_2 by 13% and MDA by 51.9% and 62.3% relative to negative control (T4). The treatments T7 and T8 further reduced the impact of effluent; however, the application of T9 and T10 decreased the H_2O_2 content by 62% and 70.2% and MDA content by 74.4% and 79%, respectively. The findings of the whole study are compared with other studies and summarized in **Table S2.** Meanwhile, these findings are consistent with Haidri et al. [66] who confirmed that ZnO-NPs has potential to reduce the impact of wastewater by decreasing oxidative stress attributes. The decrease in H_2O_2 and MDA levels with the application of nanoparticles might be due to the detoxification of ROS, which inhibits the production of hydrogen peroxide and consequently inhibits lipid peroxidation. Meanwhile, the decline in oxidative stress attributes might be due to application of ZnO-NPs which stabilize the membrane integrity and reduce oxidative damage. This study confirmed the potential of nanomaterials in strengthening the intrinsic plant defense mechanisms against wastewater stress.

View Article Online
DOI: 10.1039/D6VA00120C

During multivariate analysis, the PCA of parameters **(Fig. 8N)** showed that the growth, photosynthetic, antioxidant, and oxidative attributes had a positive relationship along the first principal component, where DIM-1 contributed approximately 91.2% and DIM-2 approximately 2.9% of the total variance. The PCA of the treatment **(Fig. 8O)** further confirmed the results, where the application of ZnO(B)-NPs and ZnO(C)-NPs clustered on the positive side towards Dim-1 and were clearly separated from the wastewater. The heat map **(Fig. 8P)** clearly shows that the application of ZnO-NPs improved the growth of *Vigna radiata*, as indicated by the red color (positive relationship), by reducing the oxidative stress attributes. The wastewater application inhibits the growth of plants by inducing phytotoxicity (blue color-negative relationship). Overall, it was observed that biosynthesized ZnO-NPs had a greater potential to reduce the phytotoxicity of textile effluent than chemically synthesized ZnO-NPs.

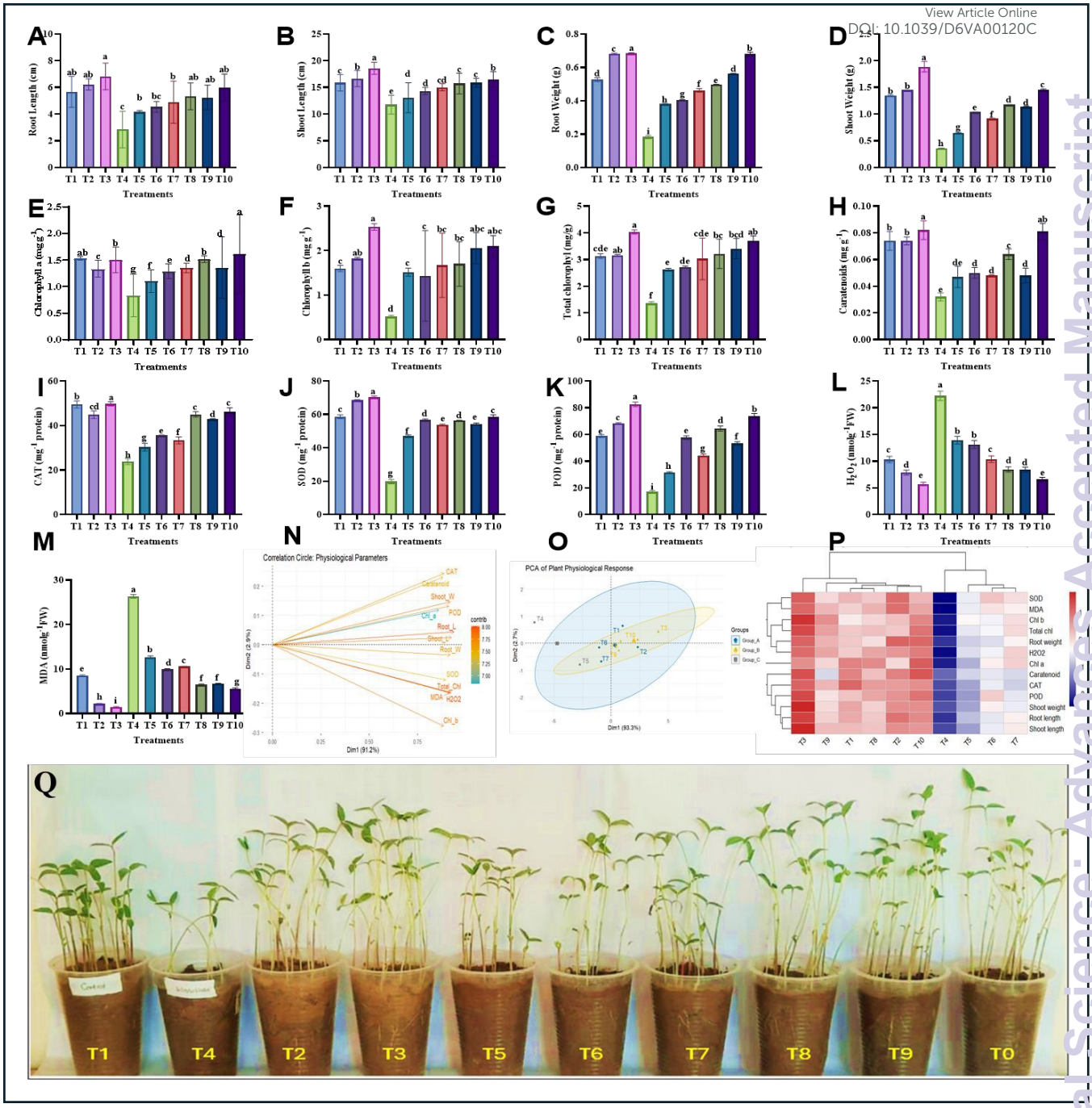

Fig. 8 Effect of different treatments on physiological and biochemical parameters of *Vigna radiata* under wastewater stress. Bar graphs represent physiological and biochemical parameters, while PCA and heatmap demonstrate the multivariant analysis. Error bars represent the standard deviation (n=3) and distinct letters show significant differences among treatments

4. Conclusion

View Article Online
DOI: 10.1039/D5VA00120C

This work focuses on the comparative analysis of bio (*Conocarpus erectus*) and chemically prepared (NaOH) ZnO-NPs for the nano-remediation of textile wastewater and reducing its phytotoxicity against *Vigna radiata*. The optimum dosage of biosynthesized ZnO-NPs (0.5 mg mL^{-1}) showed more potential and served as an environmentally friendly alternative for remediating the synthetic and actual wastewater. They reduced the color intensity, sulfate, phosphate, and COD by 72.58%, 43.54%, 79.37%, and 71.30% as compared to their chemically synthesized counterparts (2 mg mL^{-1}), which reduced the color intensity by 67.28%, sulphate by 15.75%, phosphate by 60.88%, and COD by 46.58%. Furthermore, the optimal dosages of ZnO(C) (100 mg L^{-1}) and ZnO(B) (50 mg L^{-1}) NPs showed promising bio-stimulants effect under controlled conditions, as it not only increased the germination of *Vigna radiata* but also enhanced its growth by bolstering photosynthetic efficiency (Chl content by 60% and 63% and carotenoids by 33.3% and 60.49%) and antioxidative defense mechanisms (CAT by 44% and 48.3%, SOD by 63.6% and 67%, and POD by 68.1% and 77%) against oxidative damage imposed by wastewater irrigation (Increased H_2O_2 by 53% and MDA by 67%). Therefore, this study highlights the application of ZnO-NPs for wastewater treatment and for improving plant health under wastewater stress.

Author contribution

Fatima Batool: writing – original draft, methodology, validation, formal analysis; Muhammad Zubair: methodology, writing – review & editing, visualization; Faisal Mahmood: methodology, writing – review & editing, visualization; Muhammad Shahid: methodology, formal analysis, writing – review & editing; Tanvir Shahzad: methodology, data curation, visualization; Weitao Liu: Data curation, formal analysis, validation; Aman Ullah: Investigation, methodology, validation, supervision; Sabir Hussain: Conceptualization, resources and investigation, methodology, funding acquisition, and supervision

Conflict of Interest

View Article Online
DOI: 10.1039/D6VA00120C

There are no conflicts to declare.

Consent for Publication

All authors give consent for the publication of this original article.

Acknowledgement

The authors extend their appreciation to the HEC Pakistan for funds under project number 8206/Punjab/NRPU/R&D/HEC/2017 by the Higher Education Commission of Pakistan, Government College University Faisalabad, and University of Alberta in aiding Laboratory supports.

References

1 A. Tiwari, G. S. Vishwakarma, D. Maiya, N. Kumar and A. Pandya, Engineered microbe–nanoparticle conjugates entrapped in bacterial cellulose nanopaper for sustainable, scalable and efficient textile wastewater treatment, *J. Water Process Eng.*, 2025, **77**, 108519.

2 S. Madhav, A. Ahamad, P. Singh and P. K. Mishra, A review of textile industry: Wet processing, environmental impacts, and effluent treatment methods, *Environ. Qual. Manag.*, 2018, **27**, 31–41.

3 W. U. Khan, S. Ahmed, Y. Dhoble and S. Madhav, A critical review of hazardous waste generation from textile industries and associated ecological impacts, *J. Indian Chem. Soc.*, 2023, **100**, 100829.

4 F. Batool, F. Mahmood, A. Mahmood, T. Shahzad and S. Hussain, Treatment of Textile Wastewater using Biogenic and Chemically Synthesized Iron Oxide Nanoparticles (FeO-NPs) and their Impact on Seed Germination of Vigna radiata, *Water, Air, Soil Pollut.*, 2025, **236**, 264.

5 V. S. Tanwar, S. K. Singh, J. Kumar and R. Sharma, Analysis of Properties of Municipal

View Article Online
DOI: 10.1039/D6VA00120C

Sewage Sludge and its Application: A Short Review.

6 V. S. Tanwar, S. K. Singh, J. K. Sharma and R. Patidar, Innovative Approaches to Pretreatment and Modification of Sewage Sludge-Derived Biochar for Resource Recovery: A Short Review, *J. Build. Mater. Sci. Vol.*

7 M. Zahra, G. Yasmeen, F. Aftab, H.-R. Athar, A. Saleem, S. Ambreen and M. A. Malana, ZnSe-rGO nanocomposites as photocatalysts for purification of textile dye contaminated water: A green approach to use wastewater for maize cultivation, *Heliyon*.

8 S. Sudan and J. Kaushal, Visible light promoted photocatalytic degradation of benzidine-based anionic diazo dye and its mechanistic studies using copper carbon dots incorporated biochar, *J. Mol. Liq.*, 2025, 127828.

9 R. Patidar and V. C. Srivastava, Ultrasound enhanced electro-fenton mineralization of benzophenone: kinetics and mechanistic analysis, *ACS ES&T Water*, 2022, **3**, 1595–1609.

10 S. Singh, R. Patidar, V. C. Srivastava, P. Kumar, A. Singh and S.-L. Lo, Ellipsoid-shaped copper oxide as an effective peroxymonosulfate activator for perfluorooctanoic acid decomposition, *Mater. Today Commun.*, 2023, **34**, 105107.

11 F. Batool, M. Shahid, F. Mahmood, T. Shahzad, F. Azeem, S. Hussain, T. S. Algarni, M. S. Elshikh, W. A. Al Onazi and S. Mustafa, Biosynthesis of copper nanoparticles using Bacillus flexus and estimation of their potential for decolorization of azo dyes and textile wastewater treatment, *J. King Saud Univ.*, 2024, 103309.

12 S. Mustafa, F. Mahmood, U. Shafqat, S. Hussain, M. Shahid, F. Batool, R. O. Elnour, M. Hashem, T. A. Y. Asseri and T. Shahzad, The biosynthesis of nickel oxide nanoparticles: An eco-friendly approach for azo dye decolorization and industrial wastewater treatment, *Sustainability*, 2023, **15**, 14965.

13 F. Ali, S. B. Khan, T. Kamal, K. A. Alamry and A. M. Asiri, Chitosan-titanium oxide

fibers supported zero-valent nanoparticles: Highly efficient and easily retrievable catalyst for the removal of organic pollutants, *Sci. Rep.*, 2018, **8**, 6260.

14 A. Attia, N. Elboughdiri, D. Ghernaout, B. Carbonnier, R. Ben Amar and S. Mahouche-Chergui, Enhancing the generation and stabilization of ZnO nanoparticles on modified clay with polyethylenimine to improve the photodegradation of dyes in textile wastewater, *J. Water Process Eng.*, 2025, **73**, 107711.

15 H. Yasmin, J. Mazher, A. Azmat, A. Nosheen, R. Naz, M. N. Hassan, A. Noureldeen and P. Ahmad, Combined application of zinc oxide nanoparticles and biofertilizer to induce salt resistance in safflower by regulating ion homeostasis and antioxidant defence responses, *Ecotoxicol. Environ. Saf.*, 2021, **218**, 112262.

16 V. Prakash, P. Rai, N. C. Sharma, V. P. Singh, D. K. Tripathi, S. Sharma and S. Sahi, Application of zinc oxide nanoparticles as fertilizer boosts growth in rice plant and alleviates chromium stress by regulating genes involved in oxidative stress, *Chemosphere*, 2022, **303**, 134554.

17 M. A. Nazir, M. Hasan, G. Mustafa, T. Tariq, M. M. Ahmed, R. Golzari Dehno and M. Ghorbanpour, Zinc oxide nano-fertilizer differentially effect on morphological and physiological identity of redox-enzymes and biochemical attributes in wheat (Triticum aestivum L.), *Sci. Rep.*, 2024, **14**, 13091.

18 G. Otis, M. Ejgenberg and Y. Mastai, Solvent-free mechanochemical synthesis of ZnO nanoparticles by high-energy ball milling of ε-Zn (OH) 2 crystals, *Nanomaterials*, 2021, **11**, 238.

19 D. da S. Biron, V. dos Santos and C. P. Bergmann, Synthesis and characterization of zinc oxide obtained by combining zinc nitrate with sodium hydroxide in polyol medium, *Mater. Res.*, 2020, **23**, e20200080.

20 N. M. Shamhari, B. S. Wee, S. F. Chin and K. Y. Kok, Synthesis and Characterization

of Zinc Oxide Nanoparticles with Small Particle Size Distribution., *Acta Chim. Slov.*,
View Article Online
DOI: 10.1039/D6VA00120C

21 S. Mohan, M. Vellakkat and A. Aravind, Hydrothermal synthesis and characterization of Zinc Oxide nanoparticles of various shapes under different reaction conditions, *Nano Express*, 2020, **1**, 30028.

22 A. D. Khalaji, Preparation and characterization of ZnO nanoparticles via thermal decomposition from zinc (II) Schiff base complex as new precursor, *Chem. Methodol*, 2019, **3**, 571–579.

23 D. Jain, Shivani, A. A. Bhojiya, H. Singh, H. K. Daima, M. Singh, S. R. Mohanty, B. J. Stephen and A. Singh, Microbial fabrication of zinc oxide nanoparticles and evaluation of their antimicrobial and photocatalytic properties, *Front. Chem.*, 2020, **8**, 778.

24 D. E. EL-GHWAS, Characterization and biological synthesis of zinc oxide nanoparticles by new strain of Bacillus foraminis, *Biodiversitas J. Biol. Divers.*

25 Z. S. Mahdi, F. Talebnia Roshan, M. Nikzad and H. Ezoji, Biosynthesis of zinc oxide nanoparticles using bacteria: a study on the characterization and application for electrochemical determination of bisphenol A, *Inorg. Nano-Metal Chem.*, 2021, **51**, 1249–1257.

26 C. Dias, M. Ayyanar, S. Amalraj, P. Khanal, V. Subramaniyan, S. Das, P. Gandhale, V. Biswa, R. Ali and N. Gurav, Biogenic synthesis of zinc oxide nanoparticles using mushroom fungus Cordyceps militaris: Characterization and mechanistic insights of therapeutic investigation, *J. Drug Deliv. Sci. Technol.*, 2022, **73**, 103444.

27 I. Lashin, M. Hasanin, S. A. M. Hassan and A. H. Hashem, Green biosynthesis of zinc and selenium oxide nanoparticles using callus extract of Ziziphus spina-christi: Characterization, antimicrobial, and antioxidant activity, *Biomass Convers. Biorefinery*, 2023, **13**, 10133–10146.

28 T. Gur, I. Meydan, H. Seckin, M. Bekmezci and F. Sen, Green synthesis,

characterization and bioactivity of biogenic zinc oxide nanoparticles, *Environ. Res.*, 2022, **204**, 111897.

29 S. A. Neamah, S. Albukhaty, I. Q. Falih, Y. H. Dewir and H. B. Mahood, Biosynthesis of zinc oxide nanoparticles using Capparis spinosa L. fruit extract: characterization, biocompatibility, and antioxidant activity, *Appl. Sci.*, 2023, **13**, 6604.

30 F. M. Albarakaty, M. I. Alzaban, N. K. Alharbi, F. S. Bagrwan, A. R. M. Abd El-Aziz and M. A. Mahmoud, Zinc oxide nanoparticles, biosynthesis, characterization and their potent photocatalytic degradation, and antioxidant activities, *J. King Saud Univ.*, 2023, **35**, 102434.

31 C. Zhang, J. Liu, A. Ahmeda, Y. Liu, J. Feng, H. Guan, C. Li, M. Nowrozi, M. M. Zangeneh and A. Zangeneh, Biosynthesis of zinc nanoparticles using Allium saralicum RM Fritsch leaf extract; Chemical characterization and analysis of their cytotoxicity, antioxidant, antibacterial, antifungal, and cutaneous wound healing properties, *Appl. Organomet. Chem.*, 2022, **36**, e5564.

32 R. Kothari, A. K. Pathak, V. Sharma, S. Ahmad, H. M. Singh, R. P. Singh and V. V Tyagi, Impact of pollutant load from textile dyeing industry wastewater on biometric growth profile of Vigna radiata, *Bull. Environ. Contam. Toxicol.*, 2022, **109**, 969–976.

33 A. Zgórska and A. Borgulat, Genotoxicity of wastewater samples from the textile industry detected by broad bean (Vicia faba) micronucleus test assay., *Appl. Ecol. Environ. Res.*

34 Y. Bilal, T. Sarwar, E. Mazhar, F. Mahmood, T. Shahzad, D. A. Al-Farraj, I. Alzaidi, M. S. Elshikh, T.-W. Chen and S. Hussain, Reduction in phytotoxicity of a textile wastewater against Vigna radiata using Citrobacter sp. M41 in a bioaugmented packed bed column bioreactor, *J. King Saud Univ.*, 2024, **36**, 103030.

35 Y. Bilal, M. Shahid, F. Mahmood, T. Shahzad and S. Hussain, Characterization of

View Article Online
DOI: 10.1039/D6VA00120C

rhizospheric Bacillus strains SG36 and SG42 for decolorization of reactive yellow 2 dye and Vigna radiata growth promotion in dye contaminated soil.

36 P. Das, N. Bahadur and V. Dhawan, Surfactant-modified titania for cadmium removal and textile effluent treatment together being environmentally safe for seed germination and growth of Vigna radiata, *Environ. Sci. Pollut. Res.*, 2020, **27**, 7795–7811.

37 F. Batool, F. Mahmood, T. Shahzad and S. Hussain, Ameliorating textile effluent phytotoxicity in Vigna radiate through biosynthesized Fe/Zn bimetallic nanoparticles: sustainable approach for environmental remediation, *Int. J. Environ. Sci. Technol.*, 2025, 1–16.

38 U. Shafqat, S. Hussain, T. Shahzad, M. Shahid and F. Mahmood, Elucidating the phytotoxicity thresholds of various biosynthesized nanoparticles on physical and biochemical attributes of cotton, *Chem. Biol. Technol. Agric.*, 2023, **10**, 30.

39 S. O. Ogunyemi, Y. Abdallah, M. Zhang, H. Fouad, X. Hong, E. Ibrahim, M. M. I. Masum, A. Hossain, J. Mo and B. Li, Green synthesis of zinc oxide nanoparticles using different plant extracts and their antibacterial activity against Xanthomonas oryzae pv. oryzae, *Artif. cells, nanomedicine, Biotechnol.*, 2019, **47**, 341–352.

40 A. Datta, C. Patra, H. Bharadwaj, S. Kaur, N. Dimri and R. Khajuria, Green synthesis of zinc oxide nanoparticles using parthenium hysterophorus leaf extract and evaluation of their antibacterial properties, *J. Biotechnol. Biomater*, 2017, **7**, 271–276.

41 M. Stan, A. Popa, D. Toloman, A. Dehelean, I. Lung and G. Katona, Enhanced photocatalytic degradation properties of zinc oxide nanoparticles synthesized by using plant extracts, *Mater. Sci. Semicond. Process.*, 2015, **39**, 23–29.

42 R. S. Ahmed, H. M. Hameed, M. W. Muayad, C. N. Salih, U. M. Nayef, A. A. Abed, A. M. Hussien and A. Awad, Photocatalytic Degradation of Indigo Carmine by Zinc Oxide Nanoparticles: Effect of Experimental Parameters and Kinetic Degradation, *Plasmonics*,

View Article Online
DOI: 10.1039/D6VA00120C

2025, 1–17.

43 T. Sarkar and A. Bhattacharjee, Green synthesized ZnO nanocatalysts for rapid and effective visible-light degradation of industrial dyes, *RSC Adv.*, 2026, **16**, 2671–2684.

44 H. Chelghoum, N. Nasrallah, H. Tahraoui, M. F. Seleiman, M. M. Bouhenna, H. Belmeskine, M. Zamouche, S. Djema, J. Zhang and A. Mendil, Eco-friendly synthesis of ZnO nanoparticles for quinoline dye photodegradation and antibacterial applications using advanced machine learning models, *Catalysts*, 2024, **14**, 831.

45 A. U. H. Khan, Y. Liu, R. Naidu, C. Fang, H. K. Shon, H. Zhang and R. Dharmarajan, Changes in the aggregation behaviour of zinc oxide nanoparticles influenced by perfluorooctanoic acid, salts, and humic acid in simulated waters, *Toxics*, 2024, **12**, 602.

46 S. Singh, P. Choudhary, S. Pratap, S. K. Singh, R. Patidar and A. Kumar, Mechanistic insight into photocatalytic mineralization of dyes effluent with metal oxides: Parametric optimization and kinetic study, *Water Qual. Res. J.*, 2025, **60**, 386–402.

47 S. Singh, R. Patidar, V. C. Srivastava, Q. Qiao, P. Kumar, A. Singh and S.-L. Lo, Peroxymonosulfate activation with an α-MnO2/Mn2O3/Mn3O4 hybrid system: parametric optimization and oxidative degradation of organic dye, *Environ. Sci. Pollut. Res.*, 2023, **30**, 76660–76674.

48 A. Abbas, T. Ahmad, S. Hussain, M. Noman, T. Shahzad, A. Iftikhar, Cheema, M. Ijaz, M. Tahir and G. Gohari, Immobilized biogenic zinc oxide nanoparticles as photocatalysts for degradation of methylene blue dye and treatment of textile effluents, *Int. J. Environ. Sci. Technol.*, 2022, **19**, 11333–11346.

49 D. E. Giles, M. Mohapatra, T. B. Issa, S. Anand and P. Singh, Iron and aluminium based adsorption strategies for removing arsenic from water, *J. Environ. Manage.*, 2011, **92**, 3011–3022.

50 F. Alghofaili, H. Tombuloglu, M. A. Almessiere, G. Tombuloglu, S. Akhtar, E. A.

Turumtay, A. Baykal and H. Turumtay, Phytotoxicity and growth enhancement properties of magnesium and zinc co-doped aluminum oxide nanoparticles on barley (Hordeum vulgare L.), *Environ. Sci. Pollut. Res.*, 2025, 1–21.

51 M. Kathiravan, C. Vanitha, R. Umarani, S. Marimuthu, P. Ayyadurai, K. Sathiya, M. Yuvaraj and C. Jaiby, Seed priming with biosynthesized zinc oxide nanoparticles for enhancing seed germination and vigour through promoting antioxidant and hydrolytic enzyme activity in green gram (Vigna radiata), *Agric. Res.*, 2024, 1–13.

52 A. Singh, N. áB Singh, S. Afzal, T. Singh and I. Hussain, Zinc oxide nanoparticles: a review of their biological synthesis, antimicrobial activity, uptake, translocation and biotransformation in plants, *J. Mater. Sci.*, 2018, **53**, 185–201.

53 T. C. Thounaojam, T. M. Thounaojam and H. Upadhyaya, in *Zinc-based nanostructures for environmental and agricultural applications*, Elsevier, 2021, pp. 323–337.

54 J. Razmjou, M. Mardani-Talaee and P. Vivekanandhan, Investigating the alleviatory ability of bio-synthesized zinc oxide nanoparticles from Sargassum ilicifolium (Turner) C. Agardh on the tomato plants exposed to whitefly infestation, *Sci. Rep.*, 2025, **15**, 44206.

55 A. Singh, R. S. Sengar, V. D. Rajput, T. Minkina and R. K. Singh, Zinc oxide nanoparticles improve salt tolerance in rice seedlings by improving physiological and biochemical indices, *Agriculture*, 2022, **12**, 1014.

56 W. M. Semida, A. Abdelkhalik, G. F. Mohamed, T. A. Abd El-Mageed, S. A. Abd El-Mageed, M. M. Rady and E. F. Ali, Foliar application of zinc oxide nanoparticles promotes drought stress tolerance in eggplant (Solanum melongena L.), *Plants*, 2021, **10**, 421.

57 A. Kausar, S. Hussain, T. Javed, S. Zafar, S. Anwar, S. Hussain, N. Zahra and M. Saqib, Zinc oxide nanoparticles as potential hallmarks for enhancing drought stress tolerance

View Article Online
DOI: 10.1039/D6VA00120C

in wheat seedlings, *Plant Physiol. Biochem.*, 2023, **195**, 341–350.

58 M. Rizwan, S. Ali, B. Ali, M. Adrees, M. Arshad, A. Hussain, M. Z. ur Rehman and A. A. Waris, Zinc and iron oxide nanoparticles improved the plant growth and reduced the oxidative stress and cadmium concentration in wheat, *Chemosphere*, 2019, **214**, 269–277.

59 S. R. Mousavi, Zinc in crop production and interaction with phosphorus, *Aust. J. Basic Appl. Sci.*, 2011, **5**, 1503–1509.

60 P. Ghosh and A. Roychoudhury, in *Essential Minerals in Plant-Soil Systems*, Elsevier, 2024, pp. 145–160.

61 A. Suganya, A. Saravanan and N. Manivannan, Role of zinc nutrition for increasing zinc availability, uptake, yield, and quality of maize (Zea mays L.) grains: An overview, *Commun. Soil Sci. Plant Anal*, 2020, **51**, 2001–2021.

62 J. I. García-López, G. Niño-Medina, E. Olivares-Sáenz, R. H. Lira-Saldivar, E. D. Barriga-Castro, R. Vázquez-Alvarado, P. A. Rodríguez-Salinas and F. Zavala-García, Foliar application of zinc oxide nanoparticles and zinc sulfate boosts the content of bioactive compounds in habanero peppers, *Plants*, 2019, **8**, 254.

63 H. Sturikova, O. Krystofova, D. Huska and V. Adam, Zinc, zinc nanoparticles and plants, *J. Hazard. Mater.*, 2018, **349**, 101–110.

64 A. Fathi, S. R. G. Shiade, A. Saleem, F. Shohani, A. Fazeli, A. Riaz, U. Zulfiqar, M. Shabaan, I. Ahmed and M. Rahimi, Reactive oxygen species (ROS) and antioxidant systems in enhancing plant resilience against abiotic stress, *Int. J. Agron.*, 2025, **2025**, 8834883.

65 M. Hasanuzzaman, M. H. M. B. Bhuyan, F. Zulfiqar, A. Raza, S. M. Mohsin, J. Al Mahmud, M. Fujita and V. Fotopoulos, Reactive oxygen species and antioxidant defense in plants under abiotic stress: Revisiting the crucial role of a universal defense regulator,

Antioxidants, 2020, **9**, 681.

View Article Online
DOI: 10.1039/D6VA00120C

66 I. Haidri, M. Shahid, S. Hussain, T. Shahzad, F. Mahmood, M. U. Hassan, J. M. Al-Khayri, M. I. Aldaej, M. N. Sattar and A. A.-S. Rezk, Efficacy of biogenic zinc oxide nanoparticles in treating wastewater for sustainable wheat cultivation, *Plants*, 2023, **12**, 3058.

View Article Online
DOI: 10.1039/D6VA00120C

Data Availability

Data sets generated during the current study are available from the corresponding author on reasonable request.